BIOSYSTEMS ENGINEERING 97 (2007) 145–152

Available at www.sciencedirect.com

ScienceDirect

journal homepage: www.elsevier.com/locate/issn/15375110

Research Paper: PM—Power and Machinery

A spinning-tube device for dynamic friction coefficient measurement of granular fertiliser particles

G. Kweon[a], T.E. Grift[a,*], D. Miclet[b]

[a]Department of Agricultural and Biological Engineering, University of Illinois, Urbana, IL, USA
[b]Agricultural and Environmental Engineering Research Institute (CEMAGREF), Montoldre, France

ARTICLE INFO

Article history:
Received 15 June 2006
Accepted 20 February 2007
Available online 18 April 2007

This paper describes the development of a device capable of measuring the dynamic friction coefficient of particles accelerated in a tube spinning in a horizontal plane. The dynamic friction coefficient is not the classical Coulomb friction coefficient, but a lumped parameter influenced by the Coulomb friction coefficient between particle and tube, aerodynamic effects, bouncing effects, as well as particle size, shape and texture. The principle consists of measuring the time interval associated with particles travelling through a known distance along a tube section. This time interval served as an input for a model that infers the dynamic friction coefficient.

The results for plastic spheres showed that (1) the mean dynamic friction coefficient was higher than expected (0.25), and (2) there was significant variability in the data (standard deviation (SD) 0.03) even though the particles were inserted using a precise and reproducible method.

The variability in dynamic friction coefficient was inversely proportional to the rotational velocity of the tube. This led to the conjecture that owing to the higher Coriolis forces, the particles more closely follow a straight trajectory along the inner sidewall of the tube. Owing to the lower variability, the dynamic friction coefficient measured at the highest rotational velocity (800 min^{-1}) was assumed most reliable. The mean dynamic friction coefficient of irregularly shaped potassium chloride fertiliser was measured as 0.44, SD 0.05, and for the quasi-spherical ammonium nitrate fertiliser a mean value of 0.31, with an SD of 0.03 was obtained.

1. Introduction

The popular spinner-type fertiliser spreader discharges particles after accelerating them along a vane under high centrifugal and Coriolis forces. This implies that the dynamic friction coefficient of the particle/vane combination plays an important role in the shape, throw distance, and eventual uniformity of the spread pattern. A higher dynamic friction coefficient results in particles remaining longer on the disc, which rotates the pattern in the rotational direction of the disc about its vertical axis. In addition, the particle discharge velocity will be lower, which causes particles to land closer to the spreader, reducing the spread width.

Traditionally, spinner-type fertiliser spreaders were designed for constant application rates and periodical calibration was recommended to assure proper uniformity. If, over time, the dynamic friction coefficient varies, owing to environmental changes, particle segregation or

*Corresponding author. Tel.: +1 217 333 2854; fax: +1 217 244 0323.
E-mail addresses: grift@uiuc.edu (T.E. Grift), denis.miclet@clermont.cemagref.fr (D. Miclet).
1537-5110/$ - see front matter © 2007 IAgrE. All rights reserved. Published by Elsevier Ltd
doi:10.1016/j.biosystemseng.2007.02.013

Nomenclature

A, B	integration constants
g	gravitational acceleration, $m\,s^{-2}$
R_1, R_2, R_3	sensor locations along the tube, m
t	time, s
x	distance of particle along the tube, m
$\dot{x}$	time derivative (velocity) of particle distance along the tube, $m\,s^{-2}$
$\ddot{x}$	second time derivative (acceleration) of particle distance along the tube, $m\,s^{-2}$
Δt_b	time in which a particle travels from sensor 1 to 3, s
Δt_f	time in which a particle travels from sensor 2 to 3, s
Δt_p	time during which a particle blocks sensor 2, s
κ, λ	exponential coefficients, function of Coulomb friction coefficient by definition
μ	Coulomb friction coefficient of particle along vane
ω	rotational velocity of the disc, $rad\,s^{-1}$

contamination of the spreading mechanism, serious reduction in uniformity can result. In addition, it has been shown that the basic spinner disc design is not suited for variable-rate application (Fulton *et al.*, 2001; Parish, 2002). However, since the principle of the spinner type spreader has advantages in terms of cost, capacity and maintainability, Kweon and Grift (2006) proposed the development of a feedback-controlled spinner-type fertiliser spreader based on a time-of-flight sensor developed by Grift and Hofstee (1997). This feedback-controlled spreader will include instrumentation to measure the dynamic friction coefficient in real time.

Modelling of the spreading process has been attempted over decades by researchers, such as Patterson and Reece (1962), Inns and Reece (1962), Mennel and Reece (1963), Cunningham (1963), Cunningham and Chao (1967), Brinsfield and Hummel (1975), Pitt *et al.* (1982), Griffis *et al.* (1983), Hofstee (1995), Olieslagers *et al.* (1996, 1997), Aphale *et al.* (2003), Dintwa *et al.* (2004a, 2004b), Villette *et al.* (2005). Currently, discrete element modelling is proposed as a tool to gain better insight of the spreading process, but so far no quantitative results have been obtained (Liedekerke *et al.*, 2005).

With the exception of discrete element modelling, the typical approach has been the development of differential equations describing particle motion along vanes (straight, pitched and curved) mounted on discs (flat and cone shaped). These models contain a parameter, representing the friction that the particle experiences during acceleration. To determine this constant for various materials, Aphale *et al.* (2003) and Cunningham (1963) described the measurement of the Coulomb friction coefficient using a wooden block containing fixed particles sliding along an inclined slope. Hofstee (1992) used an approach in which particles were mounted on an arm, and a spinning disc was rotating underneath it in constant contact with the particle. These methods poorly represent the complex behaviour of fertiliser particles while being accelerated under high centrifugal and Coriolis forces, influenced by the Coulomb friction coefficient between particle and vane, aerodynamic effects, bouncing effects, as well as particle size, shape and texture. To obtain more realistic values for the dynamic friction coefficient, experiments in a scenario similar to the fertiliser-spreading process are required. For instance, Villette (2005) used a machine vision approach to determine the friction angle between the radial and tangential discharge velocity components of particles that emanated from a flat disc with straight radial vanes. Although this method is indeed similar to the acceleration process on a spinner-type spreader, it is expensive, time consuming and not suitable for field application. Grift *et al.* (2006) determined the dynamic friction coefficient of a large number of urea fertiliser particles emanated from a flat disc with straight radial vanes on a commercial fertiliser spreader. Although this method is suitable for field application, more fundamental experiments with identical spheres would be costly and cumbersome. As a compromise, the spinning-tube method was developed which has the advantage that every particle leads to a measurement, allowing basic experimentation with spherical particles in a scenario similar to the fertiliser spreading process.

The objectives of this research are (1) to measure the dynamic friction coefficient of plastic spheres as well as two morphologically dissimilar fertilisers and (2) to assess whether the dynamic friction coefficient is related to the particle diameter as was found in previous research.

2. Materials and methods

The dynamic friction coefficient measurement principle is as follows: a deterministic model from the literature was adopted to describe the motion of a particle along the inner sidewall of a straight tube. This model contains a parameter, representing the friction (caused by a range of factors) that the particle experiences while being accelerated. After simplification, the differential equation was solved for the dynamic friction coefficient. The dynamic friction coefficient dictates the time required for a particle to move through a known distance. This time was measured for individual particles and used to infer their dynamic friction coefficient. Experiments were carried out for three materials, plastic spheres, ammonium nitrate fertiliser as well as potassium chloride fertiliser. Each material was tested at six rotational tube velocities and each test included 200 particles.

2.1. *Theoretical background of dynamic friction coefficient measurement*

Inns and Reece (1962) derived the differential equation for a particle sliding along a straight radial edge mounted on a disc,

while being exerted to inertia, Coriolis, centrifugal and gravity forces

$$\ddot{x} + 2\mu\omega\dot{x} - \omega^2 x = -\mu g, \tag{1}$$

where x is the distance along the edge in m as a function of time; μ is the Coulomb friction coefficient between particle and edge material; ω is the rotational velocity of the disc in rad s^{-1}, and g is the gravitational acceleration in m s^{-2}. Its absence in Eq. (1) indicates that the particle dynamics is independent of its mass. Since the downward acting gravitational force is very small compared to the horizontally acting Coriolis force, the gravity term was ignored leading to the complimentary function of Eq. (1)

$$x(t) = Ae^{\omega\kappa t} + Be^{\omega\lambda t}, \tag{2}$$

where A and B are integration constants and t is time in s. For convenience, the following 'exponential coefficients' related to the Coulomb friction coefficient were defined:

$$\begin{aligned} \kappa &= -\mu + \sqrt{\mu^2 + 1} \\ \lambda &= -\mu - \sqrt{\mu^2 + 1}. \end{aligned} \tag{3}$$

Since the Coulomb friction coefficient is positive definite, the second term in Eq. (2) always contains a negative exponential ($\lambda < 0$), whereas the first term always contains a positive exponential ($\kappa > 0$). This means that the second term vanishes quickly with time and its effect is small at a reasonable distance from the centre. In addition, since $\lambda = -1/\kappa$ and $0 < \kappa \leqslant 1$, this implies that $|\lambda| > |\kappa|$, which makes the contribution of the second term even smaller. An approximation of Eq. (3) is now (for clarity, the equal sign '$=$' is used rather than 'equal by approximation', '$\cong$')

$$x(t) = Ae^{\omega\kappa t}. \tag{4}$$

In the spinning-tube design, there are two sensors along the tube located at distances R_1 and R_2 in m, where the particle passage is detected and the corresponding time difference recorded. Assuming that at time t_1 the particle passes R_1 and at time t_2 passes R_2, substitution of these in Eq. (4) yields

$$x(t_1) = R_1 = Ae^{\kappa\omega t_1} \tag{5}$$

and

$$x(t_2) = R_2 = Ae^{\kappa\omega t_2}. \tag{6}$$

Substitution of A from Eq. (5) into (6) yields

$$R_2 = R_1 e^{\omega\kappa\Delta t}, \tag{7}$$

where, the time difference Δt between R_1 and R_2 is $t_2 - t_1$. The fact that the constant A cancels implies that the time difference Δt is independent of the boundary condition (initial drop location) but depends on the rotational velocity of the disc, ω in rad s^{-1} and the constant detection locations (R_1, R_2). Solving for the exponential coefficient κ yields

$$\kappa = \frac{\ln(R_2/R_1)}{\omega\Delta t}. \tag{8}$$

Since the Coulomb friction coefficient μ is related to κ by definition [Eq. (3)], it can be computed:

$$\mu = \frac{1}{2}\left(\frac{1}{\kappa} - \kappa\right) = \frac{1}{2}\left(\frac{\omega\Delta t}{\ln(R_2/R_1)} - \frac{\ln(R_2/R_1)}{\omega\Delta t}\right). \tag{9}$$

Although not critical, the elegant choice $R_2/R_1 = e$ simplifies Eq. (8) and (9) to

$$\kappa = \frac{1}{\omega\Delta t} \tag{10}$$

and

$$\mu = \frac{1}{2}\left(\frac{1}{\kappa} - \kappa\right) = \frac{1}{2}\left(\omega\Delta t - \frac{1}{\omega\Delta t}\right). \tag{11}$$

2.2. *Spinning-tube device*

The spinning-tube device was built using a steel tube with an inside diameter of 10 mm and an outside diameter of 14 mm. In the centre, a T connection was provided, which served as a particle insertion orifice. One side of the tube was blocked, which prevented the particle from entering the side of the tube that is not instrumented. The tube was driven by an electric motor with tachometer feedback, which allowed for accurate control of the rotational velocity. For safety, the spinning-tube device was fitted in a casing with a polycarbonate cover. Fig. 1 shows a schematic of the tube and the locations of the photo-interruption sensors. Sensor 1 was fitted at 120 mm distance from the tube centre, and sensor 2 at a distance of 241 mm. A third sensor was placed close to sensor 2 at 2.3 mm distance. The time difference between the passing of sensor 1 and 2 (Δt_b) was used to measure the dynamic friction coefficient. Similarly, the time difference between sensors 2 and 3 (Δt_f) was used to measure the discharge velocity. The combination of (Δt_f) and the total time for which the particle-blocked sensor 3 (Δt_p) was used to measure the diameter of the particles. All time differences were measured using the timer functions of a microcontroller, which was mounted directly on the spinning tube. Because of the limited storage capacity of the microcontroller, data were collected in series of 20 particles after which the machine was stopped and the data downloaded. To promote consistency, instead of simply dropping the particles into the tube, which was thought to introduce major variability due to bounce effects, they were picked up using a vacuum tube and placed in a small hole that was drilled at the bottom of the insertion orifice.

The infrared (940 nm) photo-interruption sensors have a protruding hemi-sphere, which was fitted precisely into 2 mm holes drilled in the side of the tube as shown in Fig. 2. The transmitters were spectrally matched light emitting diodes. Fig. 3 shows a photo of the spinning-tube device.

3. Results and discussion

3.1. *Experiments with identical plastic spheres*

Although the plastic spheres had a relatively constant diameter of 5.9 mm with a coefficient of variation of 1%, their measured diameters varied from approximately 5 to 6 mm as shown in Fig. 4.

This variability can be explained by assuming that the particles did not exactly follow the Coriolis force-induced straight trajectory along the sidewall of the tube, but

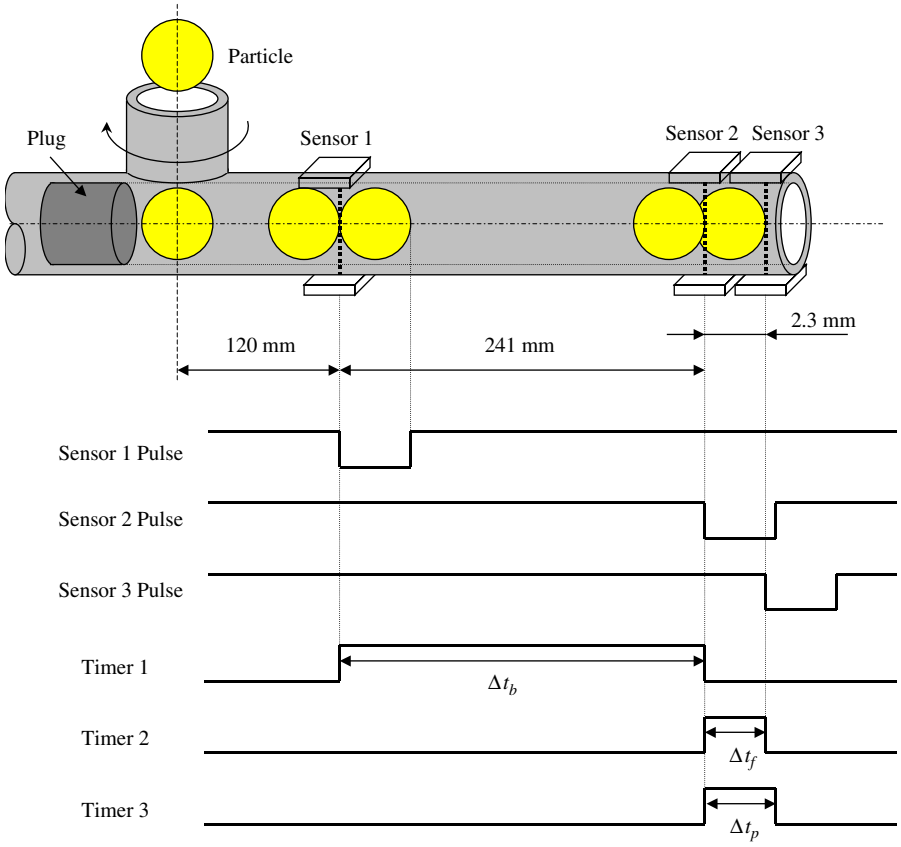

Fig. 1 – Timing signals generated by a particle passing through the tube. The particle is inserted and enters the unplugged side of the tube. When it interrupts the sensors, pulses are generated, which allow measuring the dynamic friction coefficient using Δt_b in s, the particle exit velocity in m s^{-1} using Δt_f in s, as well as the particle diameter using a combination of Δt_p in s and Δt_f in s.

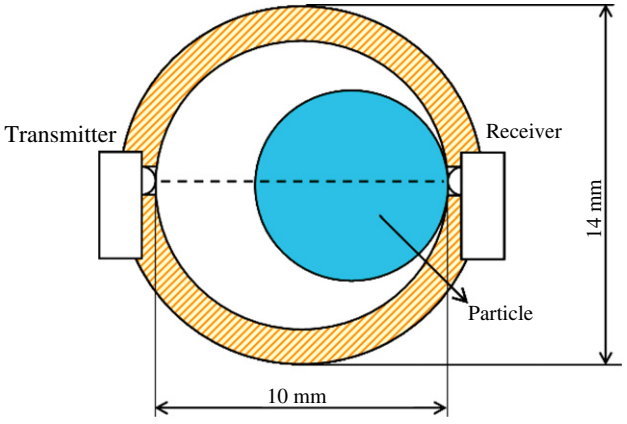

Fig. 2 – Photo-interrupter arrangement in tube to detect particle passage.

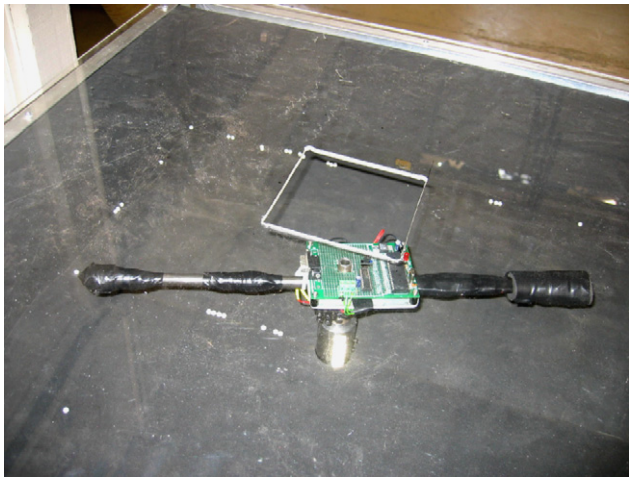

Fig. 3 – Photo of spinning-tube dynamic friction coefficient measurement device. Note the microcontroller board mounted in the centre, which spins with the tube.

oscillated around it, which implies that the sensor was not always exposed to the maximum particle dimension. This effect also implies a variation in the dynamic friction coefficient measurement; A longer time difference in passing between sensors 1 and 2, was interpreted as a higher dynamic friction coefficient, whereas in reality, the particle may have followed a longer path than assumed. Fig. 4 also shows that the variability is a function of the rotational speed, the standard deviation drops from 0.08 at 300 min^{-1} (a) to 0.03 at 800 min^{-1} (f). This adds evidence to the conjecture of the particles not following a straight trajectory along the inner

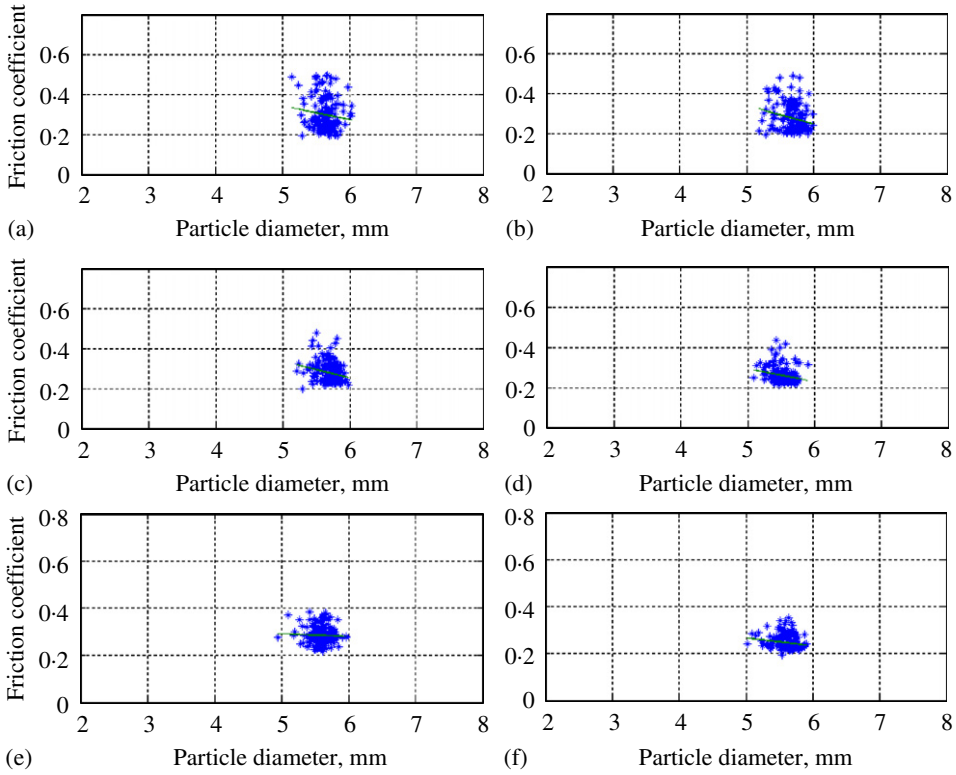

Fig. 4 – Measured dynamic friction coefficients of 200 spherical particles (5.9 mm, coefficient of variation (CV) 1%) at a tube rotational speed of (a) 300 min^{-1}, mean 0.3, SD 0.08, CV 0.27, (b) 400 min^{-1}, mean 0.28, SD 0.07, CV 0.24, (c) 500 min^{-1}, mean 0.28, SD 0.05, CV 0.18, (d) 600 min^{-1}, mean 0.26, SD 0.04, CV 0.15, (e) 700 min^{-1}, mean 0.29, SD 0.04, CV 0.13 and (f) 800 min^{-1}, mean 0.25, SD 0.03, CV 0.12.

sidewall of the tube: Higher rotational velocities exert larger Coriolis forces on the particles, resulting in the particles being pushed more firmly onto the sidewall thereby reducing the oscillation magnitude. Consequently, the most reliable value of the friction coefficient was considered at the highest velocity of 800 min^{-1}, being 0.25.

3.2. *Experiments with potassium chloride*

Experiments with potassium chloride were carried out, since this material consists mainly of flattened irregularly shaped particles with rough contours (Fig. 5).

Fig. 6 shows the measured dynamic friction coefficients of 200 potassium chloride particles again at rotational speeds ranging from 300 to 800 min^{-1}.

As in the plastic sphere case, the variability in the friction coefficients is less at higher velocities, leading to a conclusion similar to that stated in experiments with spheres: Particles are pushed more tightly onto the sidewall at higher rotational velocities. The value of the dynamic friction coefficient at the highest velocity was independent of the particle diameter being 0.44 with a standard deviation of 0.05. The latter value has to be interpreted with caution, since the oscillatory particle motion in the tube may have exaggerated the true variability as in the plastic-sphere case.

Fig. 5 – Thresholded image of potassium chloride particles with rough contours.

3.3. *Experiments with ammonium nitrate*

Ammonium nitrate is a fertiliser material, which is close to sphere as shown in Fig. 7.

Fig. 8 shows the measured dynamic friction coefficients of 200 ammonium nitrate particles at rotational speeds ranging

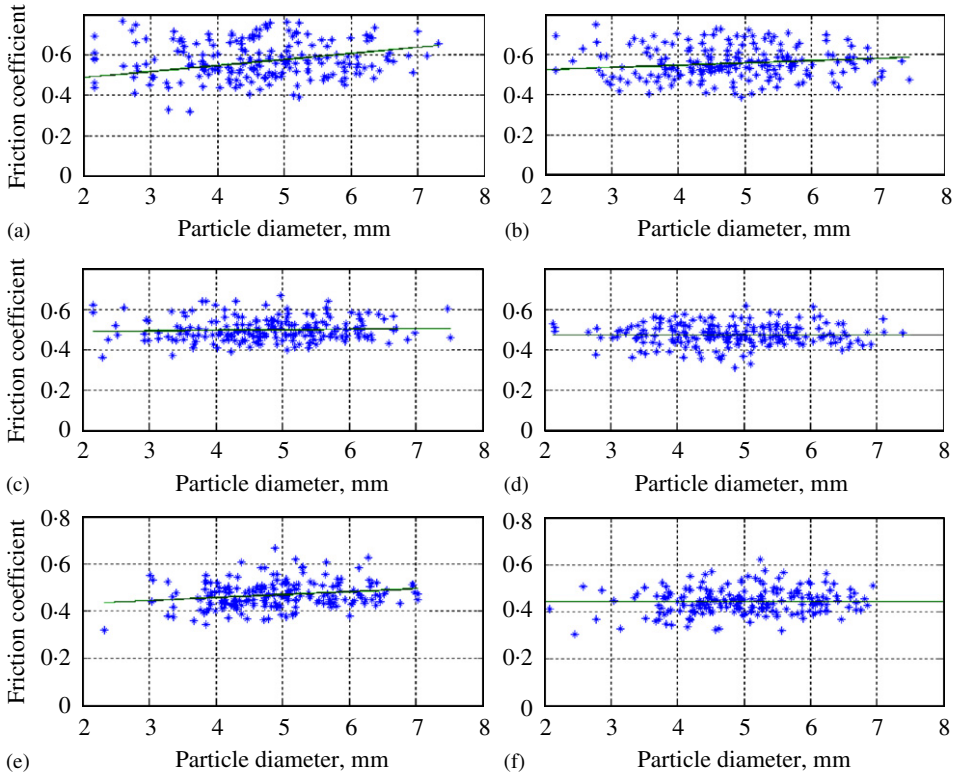

Fig. 6 – Measured dynamic friction coefficients of 200 potassium chloride particles at a tube rotational speed of (a) 300 min^{-1}, mean 0.56, SD 0.16, CV 0.29, (b) 400 min^{-1}, mean 0.54, SD 0.11, CV 0.2, (c) 500 min^{-1}, mean 0.49, SD 0.07, CV 0.14, (d) 600 min^{-1}, mean 0.47, SD 0.05, CV 0.11, (e) 700 min^{-1}, mean 0.47, SD 0.06, CV 0.14 and (f) 800 min^{-1}, mean 0.44, SD 0.05, CV 0.12.

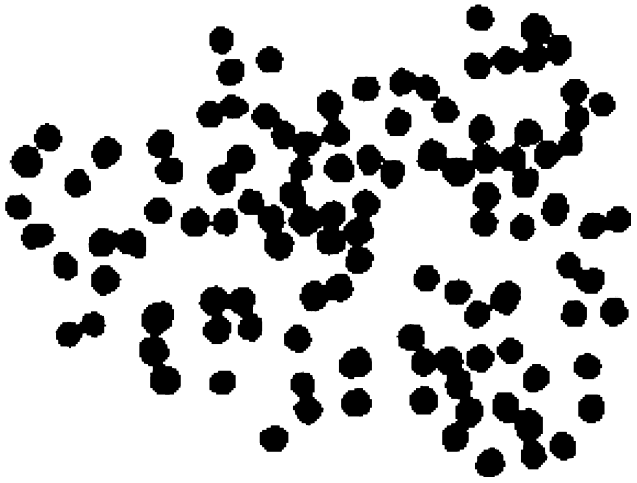

Fig. 7 – Thresholded image of ammonium nitrate particles.

from 300 to 800 min^{-1}. The value of the dynamic friction coefficient of ammonium nitrate at the highest rotational velocity (800 min^{-1}) is 0.31 and this is, expected, less than potassium chloride (0.44), and higher than that of plastic spheres (0.25). The standard deviation is in agreement with those for spheres (0.03) and is less than the value for potassium chloride, 0.05.

Previous research where the dynamic friction coefficient was measured on a spinner disc fertiliser spreader, found that the particle discharge velocity was proportional to the particle diameter and, hence, the dynamic friction coefficient was inversely proportional (Grift *et al.*, 2006). This result is not supported by the spinning-tube research where no significant relationship was found between the dynamic friction coefficient and diameter at the highest, most reliable rotational tube speeds. This implies that aerodynamic effects played a role in the previous research, since smaller particles were decelerated more during free flight than larger ones, which was incorrectly interpreted as caused by a larger dynamic friction coefficient.

4. Conclusions

A horizontally spinning-tube device that allows measuring the dynamic friction coefficient of particles was developed. Photo-interruption sensors were placed along the tube, which supplied timing information regarding particle passages from which the dynamic friction coefficients were computed using a simplified particle dynamics model. Experiments were carried out using plastic spheres, as well as ammonium nitrate and potassium chloride fertilisers.

The measured diameters and, consequently, the dynamic friction coefficients of plastic spheres showed significant variability, which led to the conjecture that particles do not exactly follow a straight trajectory along the inner sidewall of

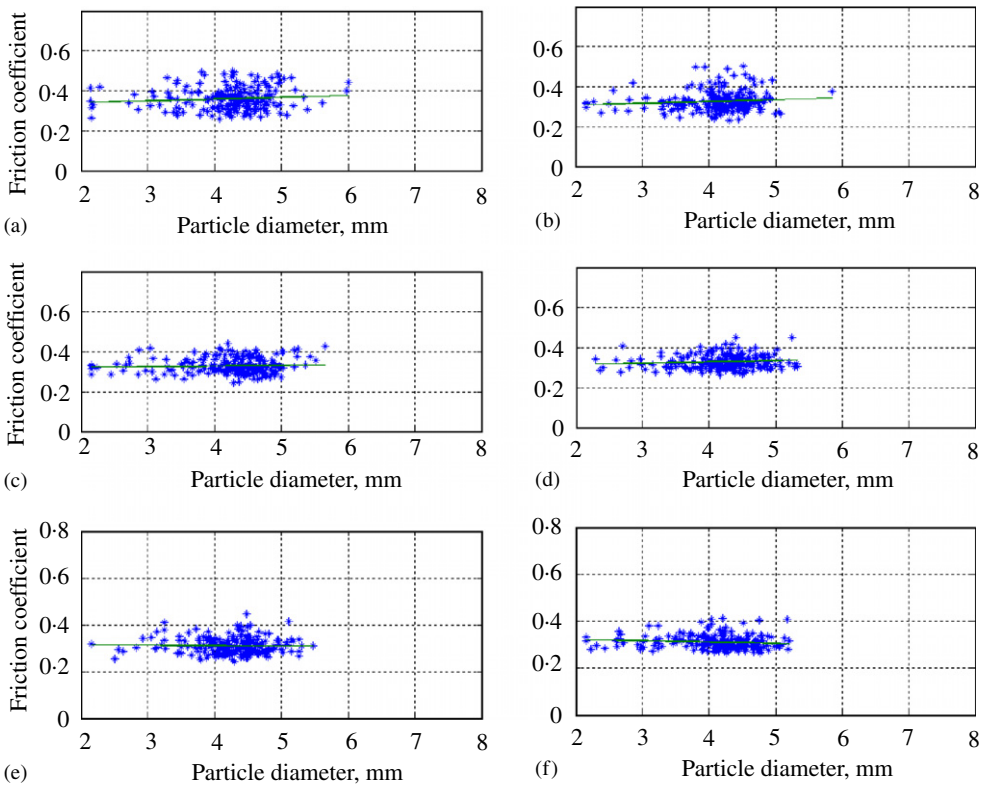

Fig. 8 – Measured dynamic friction coefficients of 200 ammonium nitrate particles at a tube rotational speed of (a) 300 min^{-1}, mean 0.36, SD 0.06, CV 0.15, (b) 400 min^{-1}, mean 0.33, SD 0.05, CV 0.15, (c) 500 min^{-1}, mean 0.33, SD 0.04, CV 0.12, (d) 600 min^{-1}, mean 0.33, SD 0.04, CV 0.11, (e) 700 min^{-1}, mean 0.31, SD 0.04, CV 0.11 and (f) 800 min^{-1}, mean 0.31, SD 0.03, CV 0.09.

the tube as expected, but rather, an oscillatory path around it. This conclusion was supported by the fact that the variability became progressively lower at higher rotational tube velocities. The assumed cause of the reduced variability was the higher Coriolis forces at higher rotational tube velocities, push the particles more firmly onto the inner sidewall of the tube, hence limit the oscillation magnitude. Therefore, the measured dynamic friction coefficients were considered most reliable at the highest rotational speeds (800 min^{-1}), leading to 0.25, standard deviation (SD) 0.03 for plastic spheres, 0.31, SD 0.03 for near-spherical ammonium nitrate and 0.44, SD 0.05 for irregularly shaped potassium chloride fertiliser.

Acknowledgements

The authors express their gratitude to all collaborators at CEMAGREF, Groupement de Clermont-Ferrand, Montoldre, France.

REFERENCES

Aphale A; Bolander N; Park J; Shaw L; Svec J; Wassgren C (2003). Granular fertiliser particle dynamics on and off a spinner spreader. Biosystems Engineering, **85**(3), 319–329, doi:10.1016/S1537-5110(03)00062-X

Brinsfield R B; Hummel J W (1975). Simulation of a new centrifugal distributor design. Transactions of the ASAE, **18**(2), 213–220

Cunningham F M (1963). Performance characteristics of bulk spreaders for granular fertiliser. Transactions of the ASAE, **6**(2), 108–114

Cunningham F M; Chao E Y S (1967). Design relationships for centrifugal fertiliser distributors. Transactions of the ASAE, **10**(1), 91–95

Dintwa E; Liedekerke P; Tijskens E; Ramon H; Olieslagers R (2004a). Model for simulation of particle flow on a centrifugal fertiliser spreader. Biosystems Engineering, **87**(4), 407–415, doi:10.1016/j.biosystemseng.2003.12.009

Dintwa E; Tijskens E; Olieslagers R; Baerdemaeker J; Ramon H (2004b). Calibration of a spinning disc spreader simulation model for accurate site-specific fertiliser application. Biosystems Engineering, **88**(1), 49–62, doi:10.1016/j.biosystemseng.2004.01.001

Fulton J P; Shearer S A; Chabra G; Higgins S F (2001). Performance assessment and model development of a variable-rate, spinner-disc fertiliser applicator. Transactions of the ASAE, **44**(5), 1071–1081

Griffis C L; Ritter D W; Matthews E J (1983). Simulation of rotary spreader distribution patterns. Transactions of the ASAE, **26**(1), 33–37

Grift T E; Hofstee J W (1997). Measurement of velocity and diameter of individual fertiliser particles by an optical method.

Journal of Agricultural Engineering Research, **66**(3), 235–238, doi:10.1006/jaer.1996.0128

Grift T E; Kweon G; Hofstee J W; Piron E; Villette S (2006). Dynamic friction coefficient measurement of granular fertiliser particles. Biosystems Engineering, **95**(4), 507–515, doi:10.1016/j.biosystemseng.2006.08.006

Hofstee J W (1992). Handling and spreading of fertilisers, part 2, physical properties of fertiliser, measuring methods and data. Journal of Agricultural Engineering Research, **53**(1), 141–162, doi:10.1016/0021-8634(92)80079-8

Hofstee J W (1995). Handling and spreading of fertilisers, part 5: the spinning disc type fertiliser spreader. Journal of Agricultural Engineering Research, **62**(3), 143–162

Inns F M; Reece A R (1962). The theory of the centrifugal distributor, II: motion on the disc, off-centre feed. Journal of Agricultural Engineering Research, **7**(4), 345–353

Kweon G; Grift T E (2006). Feed gate adaptation of a spinner spreader for uniformity control. Biosystems Engineering, **95**(1), 19–34, doi:10.1016/j.biosystemseng.2006.05.003

Liedekerke P; Tijskens E; Ramon H (2005). DEM modeling of centrifugal fertilizer spreading. First International Symposium on Centrifugal Fertiliser Spreading, 25–32 September 2005, Leuven, Belgium

Mennel R M; Reece A R (1963). The theory of the centrifugal distributor. III: Particle trajectories. Journal of Agricultural Engineering Research,, **7**(3), 78–84

Olieslagers R; Ramon H; Baerdemaeker J (1996). Calculation of fertiliser distribution patterns from a spinning disc spreader by means of a simulation model. Journal of Agricultural Engineering Research, **63**(2), 137–152, doi:10.1006/jaer.1996.0016

Olieslagers R; Ramon H; Baerdemaeker J (1997). Performance of a continuously controlled spinning disc spreader for precision application of fertiliser. In: Precision Agriculture, pp 661–668. BIOS Scientific Publishers, Abingdon, Oxfordshire, UK

Parish L R (2002). Rate setting effects on fertiliser spreader distribution patterns. Applied Engineering in Agriculture, **18**(3), 301–304

Patterson D E; Reece A R (1962). The theory of the centrifugal distributor, I: Motion on the disc, near-center feed. Journal of Agricultural Engineering Research, **7**(3), 232–240

Pitt R E; Farmer G S; Walker L P (1982). Approximating equations for rotary distributor spread patterns. Transactions of the ASAE, **25**(6), 1544–1552

Villette S (2005). Centrifugal fertiliser spreading: determination of the outlet velocity using motion blurred images. First International Symposium on Centrifugal Fertiliser Spreading, 15–16 September 2005, Leuven, Belgium

Villette S; Cointault F; Piron E; Chopinet B (2005). Centrifugal spreading: an analytical model for the motion of fertiliser particles on a spinning disc. Biosystems Engineering, **92**(2), 157–164, doi:10.1016/j.biosystemseng.2005.06.013